ADVANCED JOURNAL OF SCIENCE AND ENGINEERING
Summer 2020, Volume 1, Issue 3, Pages 91-97. DOI: 10.22034/AJSE2013091

Original Research Article

https://adv-j-sci-eng.com

eISSN: 2717-0705

An Optimized Single Motor 1 DOF Tendon-Based Transmission

Mahdi Ansari[1], Shahram Etemadi Haghighi[1,✉], Hamid Soleimanimehr[1], Mohammadreza Madanipour[1]

Received: May 17, 2020 / *Accepted*: July 09, 2020 / *Published Online*: August 08, 2020

ABSTRACT. Tendon based transmission is an efficient method for force and motion transference. Not only tendon-driven mechanisms provide dexterity and manipulability in various applications, but also they keep the structure of the mechanism light and the design delicate. Although tendon driven mechanisms are effective in driving systems with various degrees of freedom, they require either simultaneous control of parallel tendons which could be challenging or utilizing passive tendons that decreases the control over the mechanism. This paper presents a novel design for driving a planar 1 DOF joint by a single actuator. The mechanism benefits from a compound non-circular pulley which linearizes the non-linear relationship between the pulley and joint angle. The pulley enables the mechanism to operate without any controller while keeping all the tendons active which distinguishes it from the previous designs. The algorithm to derive the profile of the pulley is explained and the mechanism parameters are optimized to minimize the traction in the tendons and also to improve the precision of the mechanism. The pulley and a prototype of the mechanism have been synthesized in order to prove the authenticity of the design and to compare the test result to the algorithm outcome.

Keywords: Tendon; Motion transference; Single motor 1 DOF; Pulley.

INTRODUCTION

Tendons or in general cables are used in many mechanical devices for many years. Since the 19th century, the application of cables has been studied in robotics and hence, several tendon-actuated mechanisms have been developed. Tendon driven mechanisms (TDM) are widely used in many applications like rehabilitation robots or prosthetic hands.[1] Their lightweight structure and flexibility bring them the capability of performing complicated tasks. One of the characteristics that make the TDM special is that the actuators could be placed away from the end effector. This feature contributes to reducing the size and the weight of the mechanism and leads to a delicate design. Even though there are other types of mechanisms like parallel linkage that could be useful in similar applications,[2] their bulkiness is a drawback when size and weight are of the essence. In other cases, the combination of servo-motors and gear transmissions are used as the actuation system.[3] Although this method results in an acceptable output precision, the design bears the same downside of the parallel linkage.

Tendon traction is a unilateral force, therefore, driving TDM joints in contradictory directions requires at least a pair of tendons. There are different approaches towards handling the driving tendons in TDM. Using active and passive tendons is an effective way in designing of the under-actuated systems like bionic fingers[4] in which the passive tendons held tautly by springs. On the other hand, there are TDMs which active stiffness control systems (ASCS) are used in order to prevent slacking in the tendons.[5] Jacobsen et al. designed and developed a dexterous hand,[6] Ogane et al.[7] introduced the design and control method for a 7 DOF tendon-driven robotic arm with no linear spring tensioning devices, Kobayashi et al.[8] presented an adaptive neural network control system for TDMs with elastic tendons all utilizing ASCSs. The active stiffness control system, though effective in keeping the tendons taut could cause complexity in control methods and also, add to the computation load. Etemadi et al.[9]

✉ Corresponding author.
E-mail address: setemadi@srbiau.ac.ir (S. Etemadi Haghighi)

[1] Department of Mechanical Engineering, Science and Research Branch, Islamic Azad University, Tehran, Iran

presented a control algorithm, which can be used to control this system as well. The algorithm is suitable for nonlinear systems and uses the PSO method in inner loops. Mahmoodabadi et al.[10] proposed another control method, which also uses evolutionary algorithms inside the control loop and is capable to handle nonlinear systems like this. Both algorithms shown good performance in controlling complicated nonlinear systems.

Non-circular pulleys (NCP) could introduce non-linear behavior to the system. On the other hand, they can also be used to linearize the non-linearity present in a system. Schmit and Okada synthesized a device to realize a non-linear rotational spring from the combination of a non-circular spool and a linear translational spring.[11] They showed that for a given relation between torque and angle, there is a specific shape for the non-circular pulley to generate this function. NCPs could also be useful in situations where workspace limitations and torque capacity restrictions are present in TDM. Shin et al. exploited NCPs in combination with pneumatic artificial muscles (PAMs) to improve the position tracking performance in human-friendly robots.[12] Besides, Shin et al.[13] analyzed and introduced an optimal design strategy for circular and variable radius pulleys to improve torque capacity in systems utilizing PAMs. Endo et al.[14] developed a weight compensation mechanism with NCP and spring for an inverted pendulum. Ulrich et al.[15] proposed a method employing non-circular pulleys to accomplish passive gravity compensation. In this paper, a novel design has been introduced in order to drive a planar 1 DOF joint. A non-circular pulley has been specifically devised as a mean to steer the joint in two directions. Furthermore, the geometrical parameters of the mechanism have been optimized so that the tendons have minimum tension and the NCP profile has been derived accordingly.

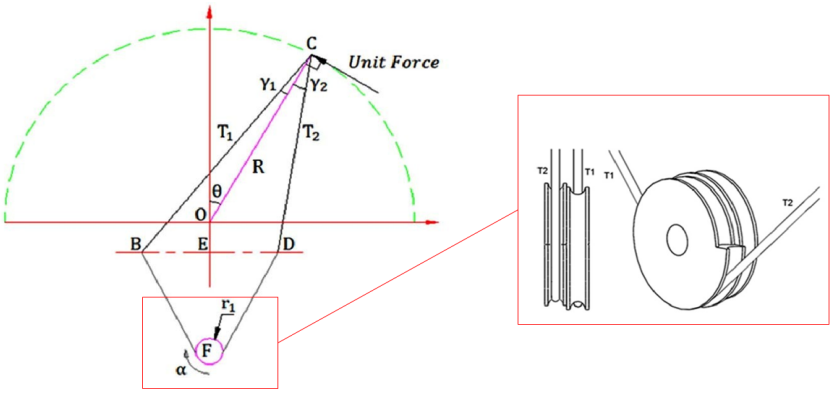

Fig. 1: The tendon-driven mechanism with the compound non-circular pulley.

Table 1: Geometrical parameters of mechanism.

Parameter	Description
R or OC	The length of the joint
BC, CD	The distance of the pins to the joint's end
EB, ED, OE, OD, EF, BG, γ_1, γ_2, φ, D, $D1$	Geometrical parameters of the mechanism
r_1	The radius of the circular pulley
r_2	The radius of the non-circular pulley at a specific α
α	Rotation angle of the pulley
θ	Rotation angle of the joint

MATERIALS AND METHODS

Mechanism Demonstration

The TDM in this paper is a 1 DOF joint driven by two tendon strings. The tendons are wounded in opposite direction around two separate pulleys which rotate together. One of the two pulleys is a regular circular one but the other one's profile is calculated according to the relationships between the geometrical parameters of the mechanism. Two small pins located at each side of the pulley, guide the tendons to be attached to the end of the 1 DOF member (OC). In this paper, the joint angle boundaries assumed to be [-30^o, $+30^o$]. Table 1 introduces the various parameters of the mechanism.

Profile Deriving Algorithm

The algorithm that derives the profile shape of the pulley is based on the geometrical analysis of the mechanism. The strategy to obtain the pulley profile is based the on segregation of the pulley rotation and the geometrical relationship between the components of the mechanism which dictates the pulley radius in each

increment of the rotation. The pulley consists of two different parts. The first part is a circular pulley with constant radius (*P1*); the second part is a non-circular pulley (*P2*) which its profile is determined by the geometry of the mechanism. These two parts rotate together as they are both attached to the same axis.

As the pulley rotates, the circular pulley releases the tendon. The length of the released tendon can be easily calculated as follows; eq. (1):

$$L = r_1 \alpha \tag{1}$$

where L is the length of the released tendon, r_1 is the radius of the circular pulley and α is the amount of pulley rotation. This length will be added to the *BC* side and consequently the joint pivots. Solving eq. (2) for theta results in the angle of the joint.

$$BC + r_1\alpha = \sqrt{(R\sin(\theta) + EB)^2 + (R\cos(\theta) + OE)^2} \tag{2}$$

The rotation of the joint deduces the length of the CD side. The length of the CD can be calculated from eq. (3).

$$CD = \sqrt{(R\sin(\theta) - ED)^2 + (R\cos(\theta) + OE)^2} \tag{3}$$

The extent of the reduction in the *CD* side equals the tendon length wounded around the non-circular pulley. The radius of this pulley in each increment of α is obtained by solving eq. (4).

$$CD_i - CD_{i-1} = r_2\,\alpha \tag{4}$$

By drawing the calculated radii respecting to the corresponding alpha, the non-circular profile of the second pulley could be revealed.

Kinetic Analysis

To obtain the tension in the tendons, a kinematic assessment has been performed. In order to model the force that the environment exerts to the *OC* member, an imaginary F_c force is considered to act at the tip of *OC*. Since *OC* is a two force member, the parallel component of the force will be neutralized by the reaction force of the *O* joint. Hence, the force is assumed to be perpendicular to the *OC* member. The equilibrium equations for the member give us the eq. (5).

$$\begin{aligned} F_c + T_1 sin(\gamma_1) - T_2 sin(\gamma_2) &= 0 \\ T_1 cos(\gamma_1) + T_2 cos(\gamma_2) - F_0 &= 0 \end{aligned} \tag{5}$$

The three unknown parameters are T_1, T_2, and F_o. Considering there are only 2 independent equations, the system is under-constrained. Since T_1 tendon acts as a resistant force to the actuator, therefore the tension in the T_1 tendon assumed to be equal to zero. This assumption is based on the fact that as a result of F_c force, a small deflection will occur in the T_2 tendon. Hence, the joint would rotate slightly in the direction of the Fc and consequently would slack the T_1 just enough to diminish the tension to zero. This assumption leaves us with only two unknowns. By Solving the equations the tension in the T_2 tendon can be can be simply calculated by eq. (6).

$$T_2 = F/sin(\gamma_2) \tag{6}$$

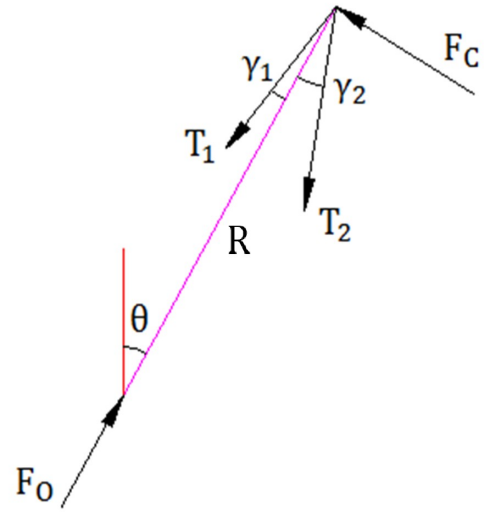

Fig. 2: The TDM joint member free body diagram.

Friction Analysis

Friction plays an important role in the performance of robotic systems. They can prompt position faults, slip-stick and various restrictions in the mechanical apparatuses. Friction analysis contributes to the better recognition of the limitations of the system and how to improve the mechanism performance.

In this project, though the friction could affect all the moving parts of the mechanism, the significant friction forces are caused by the *B* and *D* guides (Fig. 3). These guides are designed to be circular pins and the tendon could be wrapped around them to be guided to the point *C*. According to the capstan equation, the friction force of a wounded flexible line around a cylinder can be calculated by eq. (7).

$$T_b = T_a e^{\mu\varphi} \tag{7}$$

In eq. (7), T_a is the tension of the *CD* part of the tendon. This tension is equal to the force calculated in III-A and compensates the external F_c force. T_b is the tension of the *FD* part, which is wounded around the pulley and transfers the force generated by the actuator, μ is the

friction coefficient and φ is the angle swept by the tendon around the pin. As it can be inferred from the capstan equation, the friction force has an exponential relationship with the friction coefficient and also the angle swept by the tendon around the pin. As a result, the tendon tension varies with the rotation of the joint. The φ angle is obtained from eq. (8), derives the profile shape of the pulley.

$$\begin{aligned} \phi &= \pi - \measuredangle D \\ \phi &= \pi - (\tan^{-1}\frac{EF}{EB} + \sin^{-1}\frac{r_2}{BG} + \frac{\pi}{2} - \gamma_2 + \theta) \end{aligned} \quad (8)$$

Based on the capstan equation, increase in the φ angle increases the friction force exponentially. The φ angle has an inverse relationship with the D Angle. The variation of these angles could be seen in Fig. 4. The capstan equation is used to calculate the tension in the *FD* part of the tendon at every angle of the pulley.

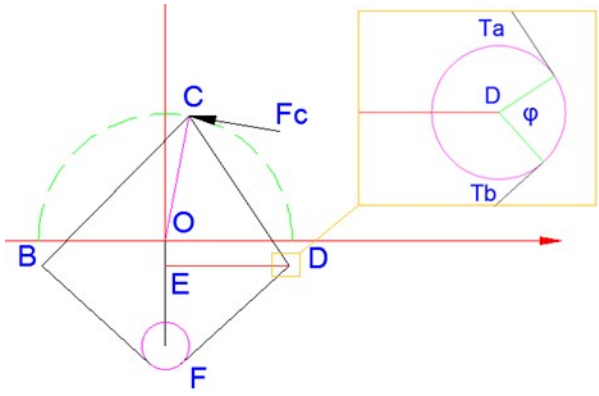

Fig. 3: Guide D orientation.

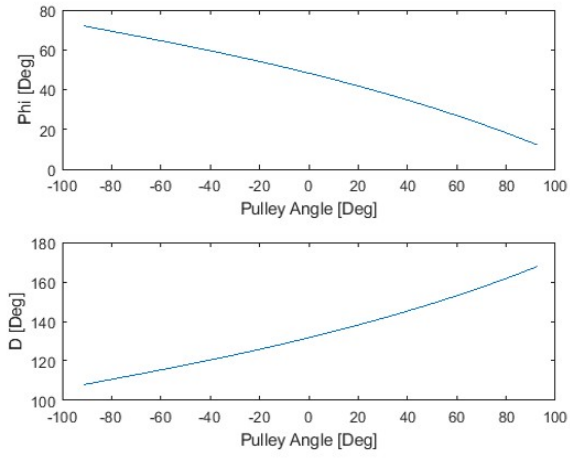

Fig. 4: The φ and D angles variation vs pulley angle.

Position Error Analysis

Elastic deformation can cause errors in mechanism such as elastic deformation error of kinematic mechanism machine tool.[16, 17] The precision of the 1 DOF joint could be affected by the deformation of different parts of the mechanism. Since this mechanism doesn't have any controller to operate, the effect of this deformation would show itself directly. Considering the fact that in this mechanism, the T_2 tendon must be flexible to operate properly and it is responsible for transmission of the force and motion, this tendon is more susceptible to deformation than other parts of the mechanism. Hence, the deformation of the other parts of the mechanism is considered negligible compared to the elongation of the tendon. The physical characteristics of the tendon are listed in Table 2.

Table 2: Physical properties of the tendon.

Parameter	Symbol	Value
Young's modulus	E	3 GPa
Diameter	D	4 mm

The extent of elongation in the tendons can be calculated by the following eq. (9).

$$\Delta = \frac{TL}{AE} \quad (9)$$

In eq. (9), T is the tension in the tendon, L is the length of the tendon, A is the cross-section area of the tendon and E is the Young's modulus. By utilizing this equation, the elongation of the tendon is illustrated vs the angle of the pulley.

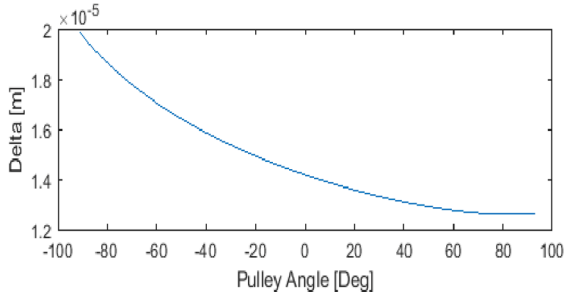

Fig. 5: T_2 tendon elongation vs pulley angle.

As it could be predicted, the elongation of the tendon diagram resembles the tension diagram of the tendon as a result of the direct relationship between these parameters. Moreover, since the length of the tendon is greater in the negative quantities of the pulley angle, the elongation graph of the tendon rises in these regions.

The elongation of the tendon causes slight rotation in the 1 DOF joint. Fig. 6 illustrates the error induced by the tendon strain. The point C shows the original position of the member's tip whereas the point C' indicates the position of the tip after tendon elongation. The extent of joint rotation as a result of this error could be derived by solving eq. (10).

$$\overrightarrow{DC'} + \overrightarrow{C'O} + \overrightarrow{OD} = 0 \quad (10)$$

Eq. (10) results in the system of eq. (11).

$$\begin{cases} -DC0\cos(D1 - \Delta D1) - C0O\sin(\theta - \Delta\theta) + ED = 0 \\ DC0\sin(D1 - \Delta D1) - C0O\cos(\theta - \Delta\theta) - OE = 0 \end{cases} \quad (11)$$

Solving the above-mentioned system of equations derives the $\Delta\theta$ which is the joint rotation error.

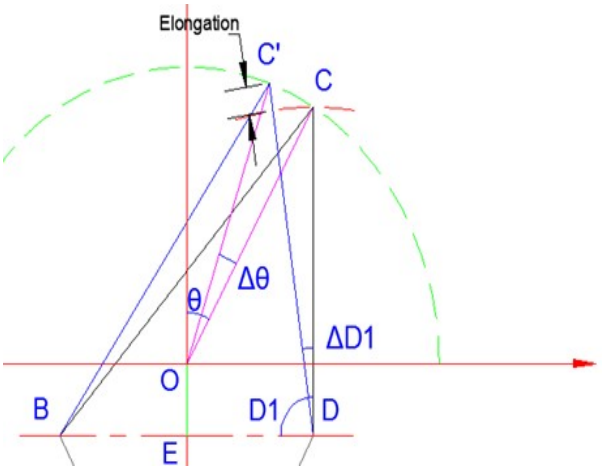

Fig. 6: The error caused by the elongation of the tendon.

Optimization

Many optimization techniques such are possible in this area while there are several considerations regarding the design of a tendon-driven mechanism.[18] These considerations depend highly on the application and limitations of the TDM which in this case, an optimum design would result in a light, dexterous and reliable TDM. To make the mechanism lighter, the actuator must be as light as possible while generating enough power. The power required by the actuator has a direct relation to the tendon tension. Hence, minimization of the tendon tension by adjusting the geometrical parameters of the mechanism is the purpose of the optimization. The above-mentioned optimization also contributes to reducing the inaccuracy of the position error and the risk of rupture in the tendons. The objective function for the optimization has been defined to be the maximum value of the tension obtained for the Tendon T_2. As its clear from the 6, the tension in T_2 has an inverse relation to the $sin(\gamma_2)$. The effective parameters on the amount of γ_2 are the lengths of *R*, *ED*, and *OE*. The boundaries assumed for the optimization procedure of these parameters are according to Table 3. These boundaries are selected based on the outcome of several executions of the algorithm to find the ranges for logical results. Since most of the applications of the TDM, like bionic hands tend to have narrow structures, a linear inequality was desirable between the *R* and *ED*.

The optimization has been conducted regarding eq. (12).

$$EB < \frac{1}{2}R \quad (12)$$

Table 3: Boundaries for effective optimization parameters

Parameter	Symbol	Lower boundary	Upper boundary
***OC* Length**	*R*	1	3
***ED* Length**	*ED*	0.3	1.5
***OE* Length**	*OE*	−0.4	0.5

The optimization has been performed using the Genetic Algorithm (GA). This algorithm has been selected because it could be used to find the global minimum value of a constrained multi-variable function. The *GA* parameters are adjusted so that the best result could be obtained within a limited number of iterations. The optimization revealed the best values for the geometrical parameters of the mechanism in order to have minimum tension in the T_2 tendon. Fig. 7 illustrates the variation of the mean value of *GA* chromosomes during 6 generations. The fitness function which is the maximum value of the tension in the T_2 tendon converged and the corresponding values for the optimization parameters has been found.

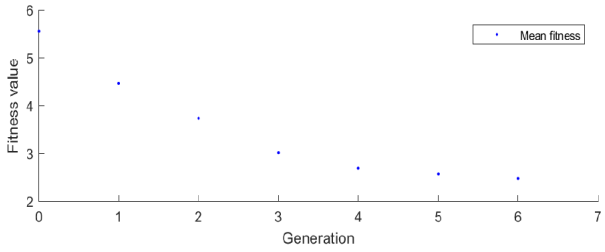

Fig. 7: The variation of the mean value of *GA* chromosomes in each generation during the optimization procedure.

RESULTS AND DISCUSSION

The profile of the NCP with the optimized parameters is illustrated in Fig. 8. The obtained values for the optimization parameters are listed in Table 4.

Table 4: Optimization results for parameters.

Parameter	Symbol	Optimum value
***OC* Length**	*R*	1.0
***ED*, *EB* Length**	*ED, EB*	0.5
***OE* Length**	*OE*	−0.4

The optimization results show that the best values for three optimization parameters are located at the boundary. The optimum value for *R* is 1 which is the

lower boundary of this parameter and as a result of the inequality condition of 12, the maximum value of the *ED* could only be equal to 0.5. The best value for *OE* is also its lower boundary. The objective of the optimization was to minimize the maximum amount of the T_2 traction. Fig. 9 illustrates the variation of T_2 tension with pulley angle.

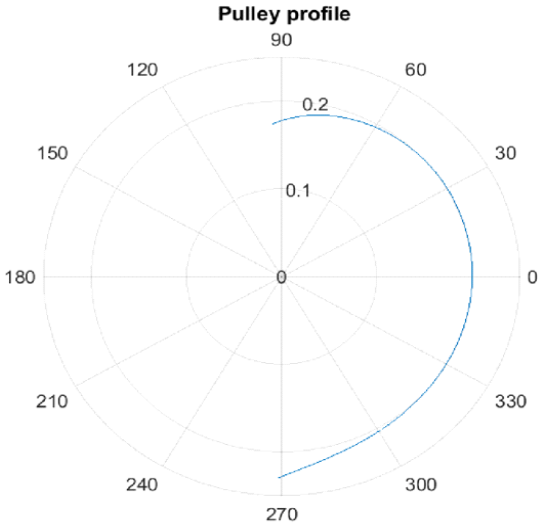

Fig. 8: The calculated optimum profile of the non-circular pulley.

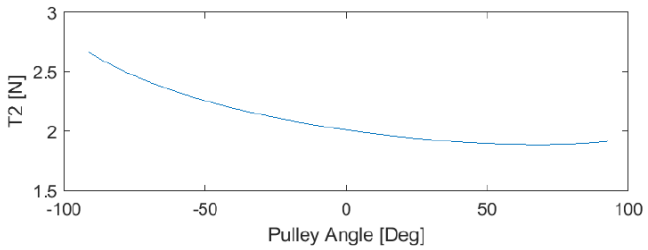

Fig. 9: The T_2 tension vs. pulley angle.

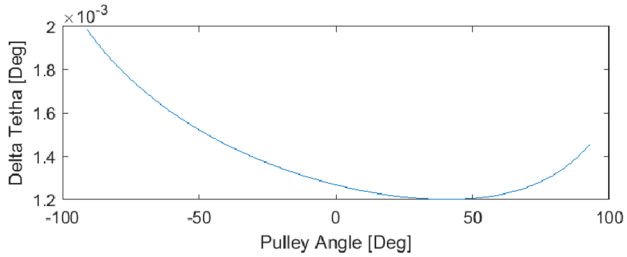

Fig. 10: Joint rotation error vs pulley angle.

The maximum tension occurs at the negative limit of the pulley angle. Based on the position error analysis, the variation of the rotation error, $\Delta\theta$, is calculated which is displayed in Fig. 10. The rotation error diagram of the joint shows that the maximum error occurs in the negative limit of the pulley angle similar to the maximum tension. In addition to that, the length of the tendon has its utmost size in this position, which makes this orientation of the mechanism critical.

The position error analysis results show that the optimization process with the objective of minimizing the tendon tension enhances the precision of the mechanism too and reduces the amount of joint position error. The optimum mechanism is illustrated in Fig. 11.

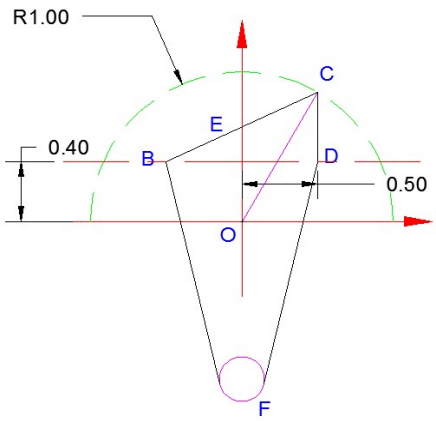

Fig. 11: The tendon-driven mechanism with the optimized parameters (*ED*, *EB* = 0.5 and *OC* = 1).

A model has been built, based on the parameters of the optimum mechanism. The mechanism pulley, as it mentioned earlier consists of a variable radius part and a circular one. Utilizing this pulley together with the optimized mechanism result in best performance with the least amount of error in the 1 DOF joint. The mechanism and the synthesized pulley (Fig. 12) have been tested for accuracy and the results from the experiment has been compared to the algorithm outcome in Fig. 13. The test results show acceptable precision throughout the course of the joint rotation.

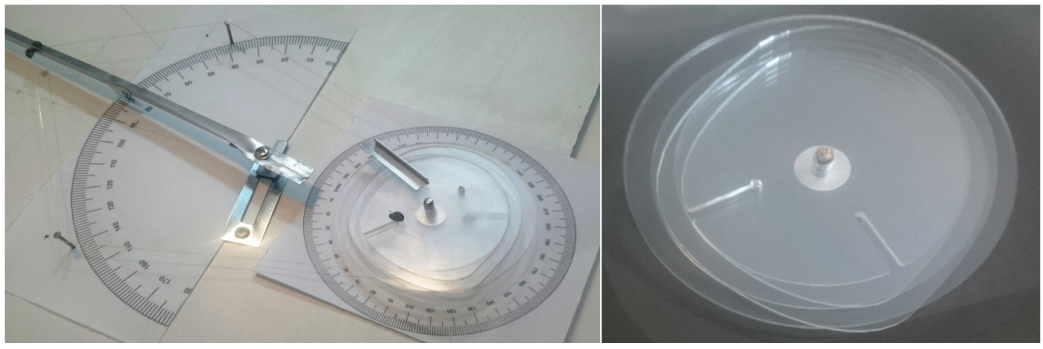

Fig. 12: The TDM test model and the synthesized compound pulley.

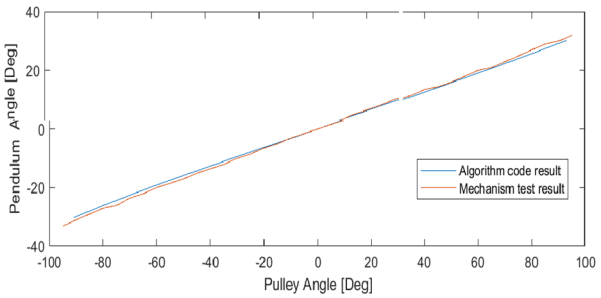

Fig. 13: The comparison of the synthesized model test result and the algorithm result.

CONCLUSION

In this paper, the design and optimization of a single motor tendon-driven mechanism have been presented. The algorithm leading to the profile of the non-circular pulley has been introduced. This design provided a methodology for linearization of the relationship between the pulley and joint angle in the TDM. The other contribution of this design is using only a single actuator without any controller to drive a 1 DOF joint while keeping both tendons active which distinguishes it from similar mechanisms. Based on the kinematics of the TDM, the effective parameters on the tendon tension have been identified. The optimization process resulted in lesser tendon tension and position error. This contributes to the performance of the mechanism as well as the attenuation of the size of the actuator. The devised TDM with the designed compound pulley have been built and the comparison between test results and the algorithm outcome showed acceptable precision and proved the authenticity of the algorithm. In future works we will try to apply control algorithm on this joint. Some previous optimization based control methods[9-10] have good potential for controlling nonlinear systems like this joint, but further studies are still required to achieve the optimum result.

REFERENCES

1. Ozawa R, Kobayashi H, Hashirii K. Analysis, classification, and design of tendon-driven mechanisms. IEEE Trans. Rob. 2013;30:396-410.
2. Birglen L, Laliberté T, Gosselin CM. Underactuated robotic hands. Springer; 2007.
3. Liu H, Meusel P, Seitz N, Willberg B, Hirzinger G, Jin MH, Liu YW, Wei R, Xie ZW. The modular multisensory DLR-HIT-Hand. Mech. Mach. Theor. 2007;42:612-625.
4. Ozawa R, Hashirii K, Kobayashi H. Design and control of underactuated tendon-driven mechanisms. IEEE Int. Conf. Rob. Auto. 2009;1522-1527.
5. Lee YT, Choi HR, Chung WK, Youm Y. Stiffness control of a coupled tendon-driven robot hand. IEEE Control Sys. Mag. 1994;14:10-19.
6. Jacobsen SC, Wood JE, Knutti DF, Biggers KB. The UTAH/MIT dextrous hand: Work in progress. Int. J. Rob. Res. 1984;3:21-50.
7. Ogane D, Hyodo K, Kobayashi H. Mechanism and control of a 7 DOF tendon-driven robotic arm with NST. J. Rob. Soc, Japan. 1996;14:1152-1159.
8. Kobayashi H, Ozawa R. Adaptive neural network control of tendon-driven mechanisms with elastic tendons. Automatica 2003;39:1509-1519.
9. Etemadi S, Vatankhah R, Alasty A, Vossoughi GR, Boroushaki M. Leader connectivity management and flocking velocity optimization using the particle swarm optimization method. Sci. Iran. 2012;19:1251-1257.
10. Mahmoodabadi MJ, Maafi RA, Haghighi SE, Moradi A. Pareto design of decoupled fuzzy sliding mode controller for nonlinear and underactuated systems using a hybrid optimization algorithm. SAIEE Africa Res J. 2020;111:4-21.
11. Schmit N, Okada M. Design and realization of a non-circular cable spool to synthesize a nonlinear rotational spring. Adv. Rob. 2012;26:234-251.
12. Shin D, Yeh X, Khatib O. Variable radius pulley design methodology for pneumatic artificial muscle-based antagonistic actuation systems. In2011 IEEE/RSJ Int. Conf. Intell. Rob. Sys. 2011;1830-1835.
13. Shin D, Yeh X, Khatib O. Circular pulley versus variable radius pulley: Optimal design methodologies and dynamic characteristics analysis. IEEE Trans. Rob. 2013;29:766-774.
14. Endo G, Yamada H, Yajima A, Ogata M, Hirose S. A passive weight compensation mechanism with a non-circular pulley and a spring. IEEE Int. Conf. Rob. Auto. 2010;3843-3848.
15. Ulrich N, Kumar V. Passive mechanical gravity compensation for robot manipulators. IEEE Int. Conf. Rob. Auto. 1991;1536-1537.
16. Soleimanimehr H, Nategh MJ. An investigation on the influence of cutting-force's components on the work-piece diametrical error in ultrasonic-vibration-assisted turning. AIP Conf. Proc. 2011;1315:1145-1150.
17. Soleimanimehr H, Nategh MJ, Jamshidi H. Mechanistic model of work-piece diametrical error in conventional and ultrasonic assisted turning. Adv. Mater. Res. 2012;445:911-916.

How to cite this article: Ansari M, Etemadi Haghighi S, Soleimanimehr H, Madanipour M. An optimized single motor 1 DOF tendon-based transmission. Adv. J. Sci. Eng. 2020;1(3):91-97.
DOI: http://doi.org/10.22034/AJSE2013091